

## PHYSICALLY INFORMED SYNTHESIS OF JACKHAMMER TOOL IMPACT SOUNDS

Sami Oksanen, Julian Parker, and Vesa Välimäki

Department of Signal Processing and Acoustics  
Aalto University, Espoo, Finland  
sami.oksanen@aalto.fi

### ABSTRACT

This paper introduces a sound synthesis method for jackhammer tool impact sounds. The model is based on parallel waveguide models for longitudinal and transversal vibrations. The longitudinal sounds are produced using a comb filter that is tuned to match the longitudinal resonances of a steel bar. The dispersive transversal vibrations are produced using a comb filter which has a cascade of first-order allpass filters and time-varying feedback coefficient. The synthesis model is driven by an input generator unit that produces a train of Hann pulses at predetermined time-intervals. Each pulse has its amplitude modified slightly by a random process. For increased realism each impact is followed by a number of repetitive impacts with variable amplitude and time difference according to the initial pulse. The sound output of the model is realized by mixing both transversal and longitudinal signals and the effect is finalized by an equalizer.

### 1. INTRODUCTION

The jackhammer sound is a familiar part of the soundscape of the city, being commonly used in both road works and on building sites. A simulation of this sound would be a useful part of the repertoire for sound designers working with audio for games or film.

The sound generation in rock or concrete breaking is caused by the main functional parts of the rock breaking device, including the power generating unit, the breaking tool, and the pneumatic devices exhaust air from the muffler [1, 2]. Typically the majority of the sound output is generated by the mechanism that is used to transmit the piston impacts as compressive pulses along the tool to the rock. The compressive pulses excite the breaking tool vibrations [3, 2, 4]. Steel bar vibrations are divided to three categories based on the nature of the wave propagation, namely longitudinal, transversal, and torsional [5]. The amount of transversal vibrations with respect to longitudinal is dependent on various phenomena [6]. Typically transversal vibrations are excited by non-parallel impacts [7]. Torsional vibrations propagate at extremely high frequencies (in the MHz range), and are not generally involved in audible sound output [8].

The approach in this paper is based in modeling the physical properties of musical instruments i.e. instruments with dispersive rigid bar vibration such as tubular bells [9, 10] or more general objects like springs which exhibit dispersive propagation [11, 12]. Digital waveguide techniques that are previously used in musical instrument modeling [13, 14] are now applied to tool sound synthesis. Some work on non-musical sound synthesis has been done e.g. in the field of automotive sound synthesis [15, 16], and various approaches by applying procedural audio methods to everyday sound sources [17], hand clapping [18], foot steps [19], and

sounding objects [20]. However, the field of machine tool sound synthesis is fairly novel. Hoffmann et al. [21] modeled surgical drill sounds with a sinusoidal model.

The scope of this paper is to introduce a sound synthesis model for jackhammer impact sounds. The proposed model has multiple parameters to adjust the sound output in order to meet the nuances of different tool constructions, operational conditions and impact parameters.

This paper is organized as follows. First, the basics of tool vibrations are discussed in Sec. 2. Then, the proposed sound synthesis method is introduced and the main functional parts are explained in Sec. 3. Next, model results are presented and discussed in Sec. 4. Finally, conclusions are drawn in Sec. 5.

### 2. TOOL VIBRATIONS

A jackhammer tool is a solid steel bar with a round or hexagonal cross-section. The size of the tool varies according to size of the jackhammer machine. Typically the tool length can vary between 30 cm to nearly 1 m and diameter varies between 15 mm to 50 mm. The longitudinal modal frequencies for steel bar are determined by

$$f_L = \frac{kc_s}{2l}, \quad (1)$$

where  $k$  is the mode index,  $c_s = 5200$  m/s is the speed of sound in steel, and  $l$  is the bar length. Hawkes and Burks [1] presented the following definition for transversal modal frequencies

$$f_T = \frac{k^2 \pi d c_s}{8l^2} \left[ 1 - 1.2 \left( \frac{kd}{l} \right)^2 \right] \left( \frac{2k+1}{2k} \right)^2, \quad (2)$$

where  $d$  is diameter of the bar. The middle term applies the Timoshenko correction at lower frequencies where modes are located at more dense intervals. The final term of the equation accounts for the boundary conditions of the bar.

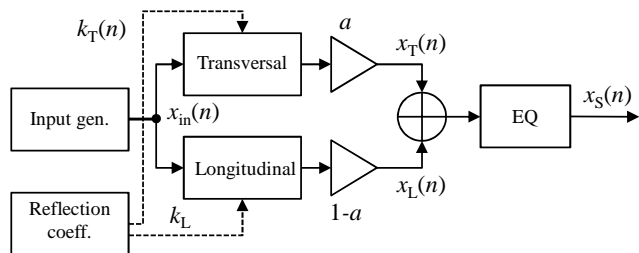


Figure 1: Jackhammer tool sound synthesis model.

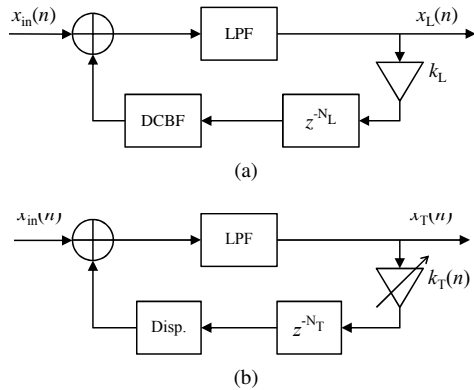


Figure 2: Synthesis units, (a) longitudinal and (b) transversal.

### 3. PROPOSED MODEL

The proposed sound synthesis model is presented in Fig. 1. The model has five main functional units, namely input generator, longitudinal vibration unit, transversal vibration unit, reflection coefficient generator for transversal unit, and equalizer. The sound output  $x_S(n)$  is a weighted sum of longitudinal  $x_L(n)$  and transversal  $x_T(n)$  output signals. The spectral balance of the model output is adjusted using an equalization filter (EQ) for summed longitudinal and transversal outputs. A first-order highpass filter ( $-6$  dB @  $800$  Hz) is used to equalize the model output to compensate for ineffective sound radiation at low frequencies. The functionality of each block is explained in more detail in the following sub-sections.

#### 3.1. Longitudinal Vibration Model

The longitudinal vibration model is based on a digital comb filter with a lowpass filter (LPF) in the feed-forward section and a delay line in feedback loop (see Fig. 2a). The longitudinal model is tuned to match the resonance frequencies (Eq. 1) of the tool by adjusting the delay line length  $N_L$ . The reflection coefficient  $k_L$  is used to adjust the desired decay time for the filter impulse response. To avoid the unwanted effects of a DC-bias in the model output, the longitudinal model has a DC-blocking filter (DCBF) [22] inside the feedback loop. The DC-blocking filter has the transfer function

$$H_{DCB}(z) = \frac{1 - z^{-1}}{1 - Rz^{-1}}, \quad (3)$$

where  $R$  is used to set desired cutoff frequency, for longitudinal model  $R = 0.995$  having the  $-6$  dB point at about  $20$  Hz.

#### 3.2. Transversal Vibration Model

The transversal vibration model is presented in Fig. 2b. It is based on a similar structure to the longitudinal model. The main difference between models is the dispersion filter (DISP) and the time-varying reflection coefficient  $k_T(n)$  in the transversal model. The time-varying reflection coefficient is used to simulate the damping of vibration that occurs whilst the excitation mechanism is in contact with the tool.

Transversal vibrations in a steel bar are strongly dispersive [5]. The approach to modeling transversal vibrations begins with the dispersion filter design process. The dispersion is modeled using a

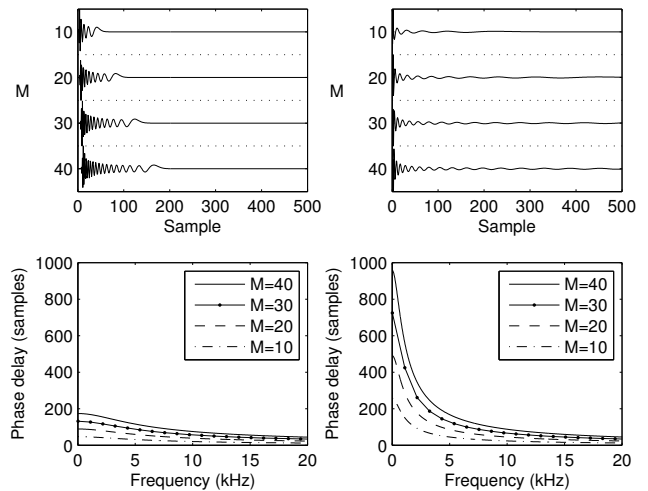


Figure 3: Dispersion filter design, impulse responses of varying length  $M$  cascade of first-order allpass filters  $\lambda = -0.618$  (top left) and with  $\lambda = -0.918$  (top right). Phase delay curves for different cascade lengths with  $\lambda = -0.618$  (bottom left) and  $\lambda = -0.918$  (bottom right).

first-order allpass filter as a prototype. The first-order allpass filter transfer function is

$$H_{AP}(z) = \frac{\lambda + z^{-1}}{1 + \lambda z^{-1}}, \quad (4)$$

where  $\lambda$  is used to adjust the filter group-delay response. In a steel bar, high-frequency transversal waves travel faster than low-frequency transversal waves, which implies that we should choose  $\lambda < 0$ . The amount of dispersion achieved using a single filter is not enough to match the dispersion characteristics of a steel bar. To increase the amount of dispersion in the model a cascade of first-order allpass filters [12, 23, 24] is used

$$H_{Cas}(z) = \left( \frac{\lambda + z^{-1}}{1 + \lambda z^{-1}} \right)^M, \quad (5)$$

where  $M$  is the cascade length.

The effect of cascade length is presented in Fig. 3 (top left) where impulse responses of cascade lengths  $M = 10 \dots 40$  are presented. The lower subplot shows corresponding phase delays for filter cascades with  $\lambda = -0.618$ . For comparison, the effect of a change in  $\lambda$  value is presented in Fig. 3 (top right), where impulse responses of filters with the different cascade lengths are demonstrated with  $\lambda = -0.918$ .

#### 3.3. Input Generation

The sound synthesis model is excited using input sequence vector  $x_{in}(n)$  containing a series of Hann pulses spaced according to the desired impact rate. The width and spacing of input pulses can be adjusted. The input pulse width affects the model output spectrum according to input pulse spectral content, i.e. wider pulses will produce less high-frequency content. Based on informal evaluation, pulse widths from  $7$  to  $11$  samples (@  $44.1$  kHz) were recognized to produce the most realistic sound output.

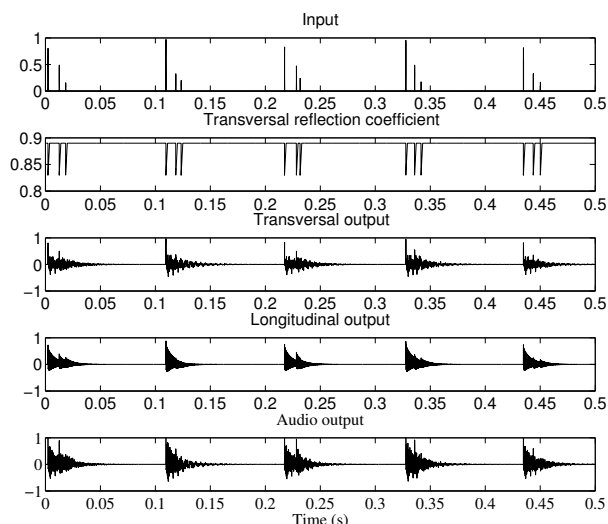


Figure 4: Synthetic time-domain signals for series of impacts.

The spacing between pulses can be set to meet the desired impact rate of the jackhammer under investigation. Typical impact rates of jackhammers can vary from 10 to 40 Hz. The amplitude of a single impact varies with each strike because of the varying state of the piston and tool. The tool could be in firm contact with the material being broken when the piston impact occurs, or there could be no contact at all.

Pulse repetitions are added to  $x_{in}(n)$  after each main impact to model the bouncing of the tool which will happen after the initial impact. The number and amplitude of the repetitions can be adjusted. The succeeding impacts are randomly spaced after the initial impact with a time difference varying from 5–10 % of the main impulse time difference. The pulse repetitions have a randomly chosen decaying amplitude. An example of a five impact series with pulse repetitions is presented in Fig. 4 (bottom). The produced input sequence is used to drive both longitudinal and transversal models.

### 3.4. Time-Varying Reflection Coefficient for Transversal Model

The input dependent time-varying reflection coefficient vector  $k_T$  for the transversal model is generated based on the excitation vector  $x_{in}(n)$ . The reflection coefficient vector  $k_T$  is initialized to value  $k_{Tmax}$ . At the beginning of each excitation pulse a linear transition ramp is generated to modulate  $k_T(n)$  value from  $k_{Tmax}$  to  $k_{Tmin}$  at a randomized slope ratio. After  $k_T(n)$  has reached  $k_{Tmin}$  an increasing ramp is generated to resume  $k_T(n)$  to  $k_{Tmax}$ . An example of  $k_T$  for single excitation pulse is presented in Fig. 5 (second from top).

## 4. RESULTS

The sound output produce by the model for single impact without pulse repetitions is presented in Fig. 5 (bottom). The input pulse length is nine samples (top),  $k_{Tmin} = 0.83$ ,  $k_{Tmax} = 0.89$ ,  $k_L = 0.94$ ,  $\lambda = -0.618$ . Output from the transversal model (middle) has a dispersive nature, the initial pulse can be distinguished from the plot but succeeding pulses are smeared in time due to dispersion. The longitudinal model output (second from bottom)

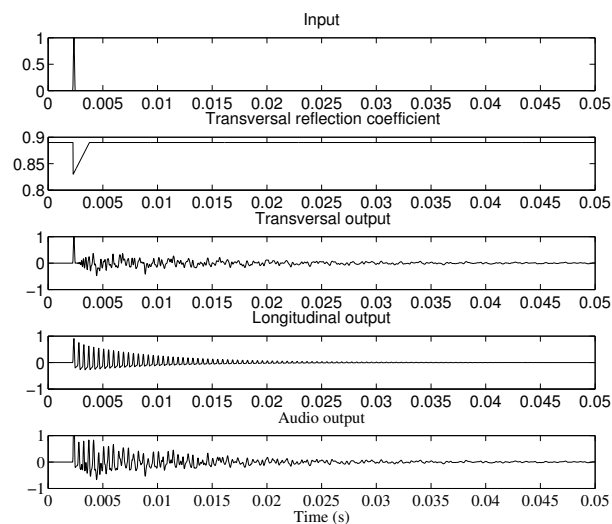


Figure 5: Synthetic time-domain signals for a single impact.

shows decaying pulse reflections, but the pulse shape of the input can still be recognized. The time-varying transversal reflection coefficient (second from top) shows the linear pulse decay in time.

Spectral plots are presented in Fig. 6. The upper subplot shows the spectrums of the longitudinal output and input signal. The transversal spectrum is presented in the middle subplot and the spectrum of the total sound output is presented in the bottom subplot. It can be seen that the spectrum of the input pulse shapes the spectral envelopes of the model outputs. Depending on the pulse duration and tool diameter there can be instances where individual modal components can vanish from the model output. For example, the mode in the longitudinal model output is seen at around 8.5 kHz in Fig. 6 (bottom).

The model output for a series of impacts in the time-domain is presented in Fig. 4 and in the spectral domain in Fig. 7. The impact rate is approxim. 10 Hz, each main impact is followed by fast repetitions at variable time intervals. The transversal reflection coefficient value is modulated by the impacts. When the repetitive impact arrives before the reflection coefficient has reached its upper threshold,  $k_{Tmax}$ , the reflection coefficient value is set to upper threshold  $k_{Tmax}$ . Examples of the audio produced by the model are available for download<sup>1</sup>.

## 5. CONCLUSIONS

A sound synthesis model for impact sounds of a jackhammer tool was presented in this paper. The model is based on the physical vibration properties of a steel bar that is excited with a series of Hann pulses. The model consists of both a longitudinal and a transversal vibration model, an input and reflection coefficient generator unit, and an equalizer. The model has various control parameters that can be used to modify the sound output according to the sound synthesis goals. The model is intended to be used as part of a procedural sound environment generation system, for use in simulators or games.

<sup>1</sup><http://www.acoustics.hut.fi/go/dafx13-impact/>

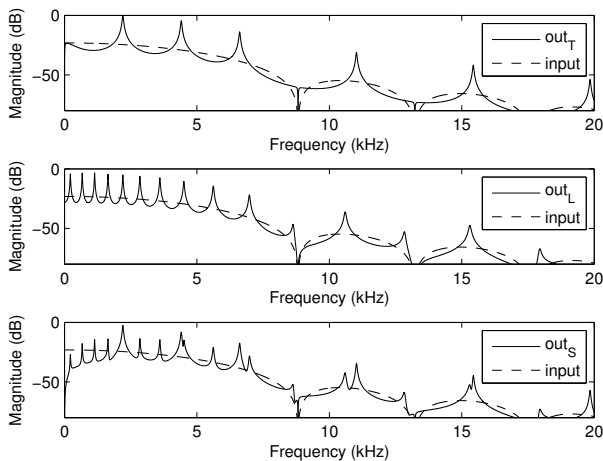


Figure 6: Signal spectrum, longitudinal (top), transversal (middle), and summed output (bottom). The spectrum of the input pulse is plotted with dashed line.

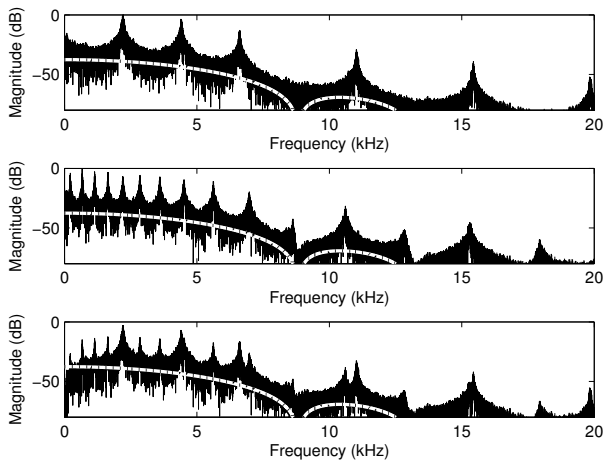


Figure 7: Signal spectrum for series of impacts, longitudinal (top), transversal (middle), and summed output (bottom). The spectrum of the input pulse is plotted with dashed line.

## 6. ACKNOWLEDGMENTS

This work was funded by the Finnish Work Environment Fund, grant no. 111244 and the GETA Graduate school.

## 7. REFERENCES

- [1] I. Hawkes and J.A. Burks, "Investigation of noise and vibration in percussive drill rods," *Int. J. Rock Mech. and Mining Sci. & Geomech. Abstr.*, vol. 16, no. 6, pp. 363–376, 1979.
- [2] J.-E. Ögren, *Noise Radiation from Drill Steels*, Ph.D. thesis, Luleå University of Technology, Luleå, Sweden, 1983.
- [3] P. K. Dutta, J. A. Burks, and R. C. Bartholomae, "Measurement and analysis of the stress wave generated rod noise in percussive rock drill," in *Proc. SESA 1981 Spring Meeting*, Dearborn, MI, USA, 1981, pp. 218–226.
- [4] A. Akay, M.T. Bengisu, and M. Latcha, "Transient acoustic radiation from impacted beam-like structures," *J. Sound and Vibration*, vol. 91, no. 1, pp. 135–145, 1983.
- [5] K. F. Graff, *Wave Motion in Elastic Solids*, Dover books on engineering. Dover Publications, 1975, Reprint 1991.
- [6] N. Dongmin, "Rigid impact – the mechanism of percussive rock drilling," in *Proc. 42nd US Rock Mech. Symp.*, San Francisco, CA, June 29th – July 2nd 2008, pp. 1–5.
- [7] V.E. Erem'yants and A.A. Slepnev, "Strain waves in colliding bars having nonparallel faces," *Journal of Mining Science*, vol. 42, no. 6, pp. 587–591, 2006.
- [8] S. Bilbao, *Numerical Sound Synthesis*, Wiley, 2009.
- [9] N. H. Fletcher and T. D. Rossing, *The Physics of Musical Instruments*, Springer-Verlag, 1991.
- [10] R. Rabenstein, T. Koch, and C. Popp, "Tubular bells: A physical and algorithmic model," *IEEE Trans. Audio, Speech, and Lang. Process.*, vol. 18, no. 4, pp. 881–890, 2010.
- [11] J. Parker, H. Penttinen, S. Bilbao, and J. Abel, "Modeling methods for the highly dispersive Slinky spring: A novel musical toy," in *Proc. DAFX-10*, Graz, Austria, Sept. 2010.
- [12] V. Välimäki, J. Parker, and J. S. Abel, "Parametric spring reverberation effect," *J. Audio Eng. Soc.*, vol. 58, no. 7/8, pp. 547–562, 2010.
- [13] J. O. Smith, "Physical modeling using digital waveguides," *Computer Music Journal*, vol. 16, no. 4, pp. 74–91, 1992.
- [14] V. Välimäki, J. Pakarinen, C. Erkut, and M. Karjalainen, "Discrete-time modelling of musical instruments," *Reports on Progress in Physics*, vol. 69, no. 1–78, pp. 1, 2006.
- [15] S.A. Amman and M. Das, "An efficient technique for modeling and synthesis of automotive engine sounds," *IEEE Trans. Industrial Electronics*, vol. 48, no. 1, pp. 225–234, 2001.
- [16] S. Cecchi, A. Primavera, L. Romoli, F. Piazza, F. Bettarelli, and A. Lattanzi, "Investigation into electric vehicles exterior noise generation," in *133rd AES Conv.*, Oct. 2012.
- [17] A. Farnell, *Designing Sound*, The MIT Press, 2010.
- [18] L. Peltola, C. Erkut, P.R. Cook, and V. Välimäki, "Synthesis of hand clapping sounds," *IEEE Trans. Audio, Speech, and Lang. Process.*, vol. 15, no. 3, pp. 1021–1029, 2007.
- [19] P. R. Cook, *Real Sound Synthesis for Interactive Applications*, AK Peters, Ltd., 1st edition, 2002.
- [20] D. Rocchesso and F. Fontana, Eds., *The Sounding Object*, Mondo Estremo, 2003.
- [21] P. F. Hoffmann, F. Gosselin, and F. Taha, "Analysis of the drilling sound component from expert performance in a maxillo-facial surgery," in *Proc. ICAD2009*, Copenhagen, Denmark, May 18–21 2009.
- [22] J. O. Smith, *Physical Audio Signal Processing*, <http://ccrma.stanford.edu/~jos/pasp/>, accessed June 17, 2013, online book.
- [23] S. A. Van Duyne and J. O. Smith, "A simplified approach to modeling dispersion caused by stiffness in strings and plates," in *Proc. ICMC 1994*, Aarhus, Denmark, 1994, pp. 335–343.
- [24] J. Rauhala and V. Välimäki, "Dispersion modeling in waveguide piano synthesis using tunable allpass filters," in *Proc. DAFX-2006*, Montreal, Canada, 2006, pp. 71–76.